

Propagation of Extremely-high Energy Leptons in the Earth: Implications to their detection by the IceCube Neutrino Telescope

Shigeru Yoshida,^{*} Rie Ishibashi,[†] and Hiroko Miyamoto
Department of Physics, Faculty of Science, Chiba University
Chiba 263-8522, Japan

(Dated: February 7, 2020)

We present the results of numerical calculations on propagation of Extremely-high energy (EHE) neutrinos and charged leptons in the earth for trajectories in all phase space of nadir angles. Our comprehensive calculation has shown that not only the secondary produced muons but also taus survive without decaying in energy range of 10PeV-100PeV with intensity approximately three orders of magnitude lower than the neutrino flux regardless of EHE neutrino production models. They form detectable horizontal or downgoing events in a 1km³ underground neutrino telescope such as the IceCube detector. The event rate and the resultant detectability of EHE signals in comparison with the atmospheric muon background are also evaluated. The 90 % C.L. upperlimit of EHE neutrino fluxes by a km² detection area would be placed at $E^2 dF/dE \simeq 3.7 \times 10^{-8}$ GeV/cm² sec sr for ν_μ and 4.6×10^{-8} for ν_τ with energies of 10⁹ GeV in absence of signals with energy-loss in a detection volume of 10PeV or greater.

PACS numbers: 98.70.Sa, 95.85.Ry, 98.70.Vc, 98.80.Cq

I. INTRODUCTION

It is well known that there exist extremely high energy (EHE) particles in the Universe with energies up to $\sim 10^{20}$ eV [1]. These EHE cosmic rays (EHECRs) may be originated in and/or producing neutrinos by the various mechanism. For example collisions of EHECRs and CMB photons photoproduce cosmogenic neutrinos [2], a consequence from the process known as the Greisen-Zatsepin-Kuzmin (GZK) mechanism [3]. Possible production of EHECRs in the present Universe due to the annihilation or collapse of topological defects (TDs) such as monopoles and/or cosmic strings [4] could also generate EHE neutrinos with energies even reaching to the GUT scale [5, 6]. EHE neutrinos provide, therefore, an unique probe to explore ultra-high energy Universe, which is one of the center piece of high energy neutrino astrophysics.

It has been argued that underground neutrino telescopes being operated and/or planned to be built are capable of detecting such EHE neutrinos [7]. In their travel in the earth to the detection volume in a telescope, EHE neutrinos collide with nuclei in the rock due to enhancement of the cross section at EHE range and produce secondary leptons like muons and taus. The expected mean free path is $\sim 600(\rho_{rock}/2.65\text{g cm}^{-3})^{-1}(\sigma_\nu/10^{-32}\text{cm}^2)^{-1}$ km which is by far shorter than a typical path length of the propagation in the earth. Moreover, the decay lifetime is long enough at EHEs for the produced μ and τ to survive and possibly reach the detection volume directly. Successive reactions of the interactions and decaying are

likely to occur in their propagation and the propagation processes of EHE particles are rather complex. The accurate understanding of the EHE neutrino and charged lepton propagation in the earth is, thus, inevitable for EHE neutrino search by underground neutrino telescopes.

There have been considerable discussions in the literature from this point of view. In the Ref. [8], the transport equations mainly focusing on ν_τ and τ were solved and the resultant particle fluxes after the propagation have been shown for trajectories of several nadir angles in the horizontal directions such as 85°. It is true that a major fraction of EHE τ tracks are coming from the horizontal directions because the earth is opaque for EHE neutrinos, but a km³ scale neutrino observatory like IceCube is essentially a 4π detector with comparable sensitivities to both muons and taus, and calculation of EHE particle energy spectra of both muons and taus over all solid angle space including downward event trajectories would be important to evaluate detectability with reasonable accuracy. Furthermore, they utilized the often-used continuous energy loss (CEL) approximation that follows only the leading cascade particles. It is a good approximation for taus, but the secondary particle fluxes contributed from the non-leading particles are not negligible for muons at EHEs where their decay does not play a visible role. Calculations on the earth-skimming EHE ν_τ have also been made in some details [9]. They used approximations to neglect contributions of generated leptons from tau interactions in the earth, which would be valid enough for consideration of earth-skimming neutrino-induced air showers. More accurate estimation of energy spectrum and contributions from particles not only skimming but propagating deeper in the earth are essential to an underground-based neutrino observatory, however.

In this work, we numerically calculate the intensity and the energy distribution of EHE neutrinos and their sec-

^{*}Electronic address: syoshida@hepburn.s.chiba-u.ac.jp;
 URL: <http://www-ppl.s.chiba-u.jp/~syoshida>

[†]Now at Ushio Denki, Co.Ltd.

ondary produced μ 's and τ 's during the propagation in the earth for the application to a km^3 scale neutrino observatory. The resultant fluxes are shown as a function of nadir angles from downward to upward going directions. All the relevant interactions are taken into account and we follow *all* produced particles in the reactions whereas the CEL approximation follows only the leading cascade particles. The initial flux is mainly assumed to be a bulk of the cosmogenic neutrinos, generated from the decay of pions photoproduced by EHE cosmic ray protons colliding with the cosmic thermal background photons, since the cosmogenic neutrino model is appropriate for a benchmark as the flux prediction is on the solid theoretical foundation. Its implications to the detection by the IceCube neutrino telescope [10], which are currently under construction at Antarctica, are then discussed in some details.

The paper is outlined as follows: First we briefly review the interactions/decay channels involved with EHE particle propagation in the earth in Sec. II. The method of our numerical calculations is also briefly explained. In the Sec. III we show the calculated results: energy distributions and intensities of muons, taus, and neutrinos after their propagation. The energy spectra of these EHE particles are shown for the cosmogenic neutrino model. Implications on the detection by the IceCube neutrino telescope are discussed in the Sec. IV and the detectability considering the possible background in the experiment is discussed in detail. The sensitivity to EHE neutrino fluxes by a km^3 neutrino observatory is also shown. We summarize our conclusions and make suggestions for future work in Sec. V.

II. DYNAMICS OF THE PROPAGATION IN THE EARTH

EHE neutrinos during the propagation do not penetrate the earth but are involved in charged/neutral current interactions that generate charged leptons and hadronic showers because their cross sections are expected to be enhanced in the ultra-high energy regime. Secondary produced μ 's and τ 's travel in the earth initiating many radiative reactions to lose their energy. The higher-order interactions like μ^\pm pair production [11] and the charged current disappearance reactions like $\mu N \rightarrow \nu_\mu X$ would regenerate charged leptons and neutrinos which are subject to further interactions. Moreover, the τ 's decay channels like $\tau \rightarrow \nu_\tau \mu \nu_\mu$ regenerate ν_τ . A primary EHE neutrino particle, therefore, results in number of particles with various energies and species which would be passing through an instrumented volume of an underground neutrino telescope. The resultant energy spectra and their intensity are consequences from the chain processes of interactions and decay. Table I summarizes the interaction/decay channels as a function of primary and generated particle species. Main energy loss process for secondary produced μ 's and τ 's are, e^\pm

TABLE I: Interactions and decay channels involved in the EHE particle propagation in the earth. Rows are primary and columns are generated particles.

	ν_e	ν_μ	ν_τ	e/γ	μ	τ	hadron
ν_e	NC ^a			CC ^b			CC/NC
ν_μ		NC			CC		CC/NC
ν_τ			NC			CC	CC/NC
μ	D ^c	D/CC		P ^d /B ^e /D	P	P	PN ^f /CC
τ	D	D	D/CC	P/B/D	P/D	P	PN/CC/D

^aNeutral Current interaction.

^bCharged Current interaction.

^cDecay.

^dPair Creation.

^eBremsstrahlung.

^fPhotonuclear interaction.

pair creation, Bremsstrahlung, and the photonuclear interactions. The relevant cross sections are formulated in Ref. [12] for pair creation, Ref. [13] for Bremsstrahlung, Ref. [14] for photonuclear interaction. Among them the photonuclear cross section has the largest theoretical uncertainty because it relies on the details of the nuclei structure function, which has to be estimated from extrapolation from the low energy data. In the present calculation is used the estimation based on the deep-inelastic scattering formalism with the ALLM parameterization of the structure function [15], which has been considered to be most reliable prediction. We artificially switch off the photonuclear interaction to see its systematic uncertainty in the results later in this paper. Furthermore, the weak interaction, $l^\pm N \rightarrow \nu X$, to cause muon and tau disappearances, and the heavier lepton pair production such as $\mu^+\mu^-$ [11] are also taken into account in the present calculation, which leads to a visible contribution to the particle fluxes at EHEs.

An EHE neutrino is a subject to charged-current (CC) and neutral-current (NC) interactions with nucleon. As there is no direct measurement of the relevant interactions in EHE range, the predictions of the νN cross sections rely on incompletely tested assumptions about the behavior of parton distributions at very small values of the momentum fraction x . Since we do not have further clues to investigate EHE neutrino interactions in our hands, we limit our present analysis within the range of the standard particle physics and use the cross section estimated by Ref. [16] using the CTEQ version 5 parton distribution functions [17].

Decay processes are also major channels and compete with the interaction processes depending on energy. The μ and τ -leptonic decay distribution can be analytically calculated from the decay matrix using the approximation that the generated lepton mass is negligible compared to that of the parent lepton [18]. For $z = E_{\nu_l}/E_l$ ($l = \mu$ or τ) it is written by

$$\frac{dn}{dz} = \frac{5}{3} - 3z^2 + \frac{4}{3}z^3 - \left(\frac{1}{3} - 3z^2 + \frac{8}{3}z^3 \right), \quad (1)$$

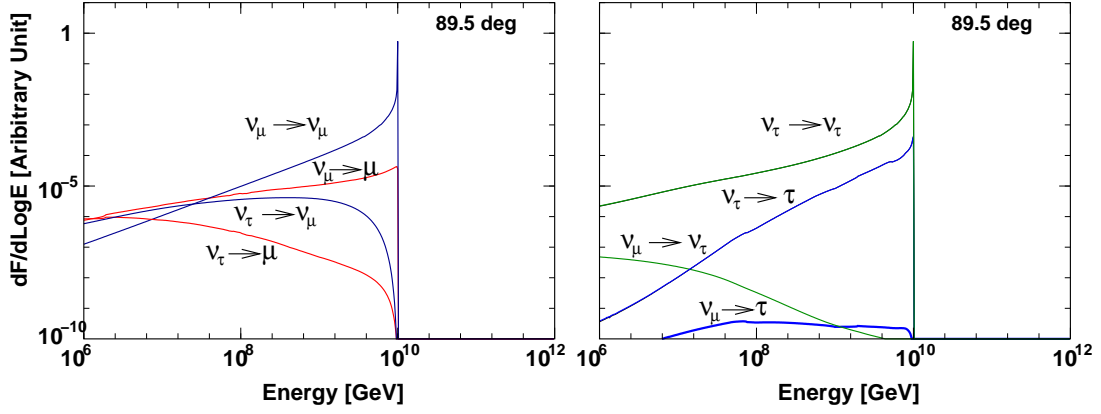


FIG. 1: The energy distribution of EHE leptons after propagation in the earth with nadir angle of 89.5 degree. μ 's and τ 's are secondary produced. The left panel shows the distributions of leptons with μ flavor while the right panel shows the case of τ flavor. Input spectrum is 10^{10} GeV monochromatic of ν_μ and ν_τ with equal intensity of "1" in this arbitrary unit.

and for $y_\nu = E_{\nu_e}/E_\mu$ (μ decay), $E_{\nu_{e,\mu}}/E_\tau$ (τ decay),

$$\frac{dn}{dz} = 2 - 6y_\nu^2 + 4y_\nu^3 - (-2 + 12y_\nu - 18y_\nu^2 + 8y_\nu^3). \quad (2)$$

The hadronic τ decay has various mode and its accurate treatment is rather difficult. Here we use the 2-body decay approximation as in Ref. [19].

The transport equations to describe the particle propagation in the earth are given by

$$\begin{aligned} \frac{dJ_\nu}{dX} = & -N_A \sigma_{\nu N, CC+NC} J_\nu + \frac{m_l}{c\rho\tau_l^d} \int dE_l \frac{1}{E_l} \frac{dn_l^d}{dE_\nu} J_l(E_l) \\ & + N_A \int dE'_\nu \frac{d\sigma_{\nu N, NC}}{dE_\nu} J_\nu(E'_\nu) \\ & + N_A \int dE'_l \frac{d\sigma_{lN, CC}}{dE_\nu} J_l(E'_l) \end{aligned} \quad (3)$$

$$\begin{aligned} \frac{dJ_l}{dX} = & -N_A \sigma_{lN} J_l - \frac{m_l}{c\rho\tau_l^d E_l} J_l \\ & + N_A \int dE'_\nu \frac{d\sigma_{\nu N, CC}}{dE_l} J_\nu(E'_\nu) \\ & + N_A \int dE'_l \frac{d\sigma_{lN}}{dE_l} J_l(E'_l) \\ & + \frac{m_l}{c\rho\tau_l^d} \int dE'_l \frac{1}{E'_l} \frac{dn_l^d}{dE_l} J_l(E'_l), \end{aligned} \quad (4)$$

where $J_l = dN_l/dE_l$ and $J_\nu = dN_\nu/dE_\nu$ are differential fluxes of charged leptons and neutrinos, respectively, N_A is the Avogadro's number, ρ is the local density of the medium (rock/ice) in the propagation path, σ is the relevant interaction cross sections, dn_l^d/dE is the energy distribution of the decay products which is derived from the decay rate per unit energy and given by Eqs. 1 and 2, c is the speed of light, m_l and τ_l^d are mass and the decay life time of the lepton l , respectively. The density profile of the rock, $\rho(L)$, is given by the Preliminary Earth Model [20]. A column density X is defined by $X = \int_0^L \rho(L') dL'$.

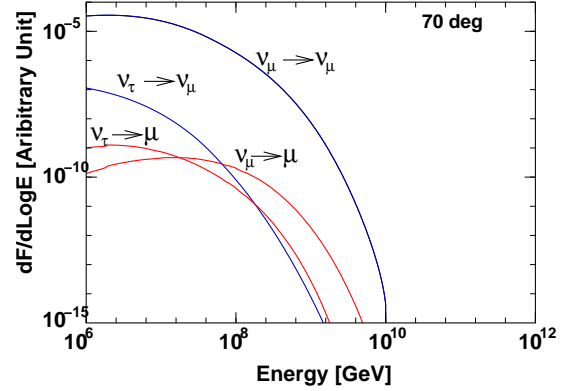


FIG. 2: Same as Fig. 1, but for nadir angle of 70 degree. The distributions of leptons with μ flavor when the input ν_μ and ν_τ is monochromatic energy of 10^{10} GeV are shown.

Eq. 3 describes the neutrino propagation. The first term is a loss due to the neutrino interaction, the second represents a contribution due to the decay, the rest of the terms accounts generation of neutrinos by the neutrino and charged lepton interactions. The fourth term represents the neutrino appearance by the CC interactions such as $\mu N \rightarrow \nu_\mu X$. Eq. 4 describes the charged lepton propagation and has the similar terms with those of Eq. 3, but also the term to represent a loss due to the lepton decay.

We numerically calculated these equations by building the matrices describing the particle propagation over infinitesimal distance as described in Ref [21, 22]. The energy differential cross sections are derived from the ones for the inelasticity parameter $y = 1 - E'/E$, i.e., $d\sigma/dy$. Let us show two examples to show the behavior of the EHE particle propagation in the earth. Fig. 1 shows the energy distribution of EHE leptons after propagation in the earth entering with nadir angle of 89.5°. The corresponding propagation distance in the earth is ~ 110 km. Primary input spectrum is monochromatic energy

distribution of 10^{10} GeV of ν_μ and ν_τ with equal intensity. Sizable bulks of the secondary produced μ 's and τ 's are found. As the μ bulk from ν_τ are mainly generated from τ decay which occurs less frequently in high energy region, their intensity decreases with higher energy. For the same reason, the secondary τ 's energy distribution is harder than that of μ 's. Note that τ originated in primary ν_μ denoted as $\nu_\mu \rightarrow \tau$ in the right panel in the figure are produced in heavy lepton pair creation $\mu \rightarrow \mu\tau^+\tau^-$.

The intensities of “prompt” muon and tau, whose energies are approximately same with the primary neutrinos, are four to five order of magnitude lower than the primary neutrino flux as indicated in the figures, but low energy bulk of the secondary muon and tau which has suffered energy loss during their propagation makes significant contribution to the flux for a given neutrino energy spectrum. It should also be remarked that the muons generated from secondary produced tau decay denoted as $\nu_\tau \rightarrow \mu$ constitute a major fraction of the intensity below 10^8 GeV. We see in the next section that they form a sizable flux for the EHE neutrino model producing hard energy spectrum like the cosmogenic neutrinos generated by the GZK mechanism.

When particles are propagating more vertically upward going, *i.e.* their propagation distance is longer, all the prompt component disappears and no particles essentially survive in EHE range, because of the significant energy losses. A typical case is shown in Fig. 2 for nadir angle of 70 degree. One can see that most bulk of the secondary muons and neutrinos are absorbed and remain only in low energy range.

Energy distributions and their intensities of EHE particles propagating in earth are, consequently, strongly dependent on the zenith (or nadir) angle of the trajectory, and also on the initial neutrino energy spectrum. One must solve the transport equation in the entire phase space in the zenith angle in order to make accurate estimations of fluxes we see in an underground neutrino telescope for a given neutrino initial flux.

III. THE COSMOGENIC NEUTRINO FLUX AT UNDERGROUND DEPTH

In this section, we discuss the case when the initial fluxes of ν_μ and ν_τ are given by the GZK mechanism, EHE neutrino production by collisions of EHECRs to CMB photons in extragalactic space, as this model has been thought to be most conventional mechanism to generate EHE neutrinos without new physics and/or speculative assumptions. The biggest uncertainty in the intensity of the cosmogenic fluxes is related to the cosmic ray source distributions. Assuming the homogeneously distributed astrophysical sources, however, variations of the magnitude of the neutrino flux above 10^9 GeV are restricted approximately within a factor of 10 [23]. Although assuming extremely hard cosmic ray injection spectrum like $\sim E^{-1}$ or very strong source evolution al-

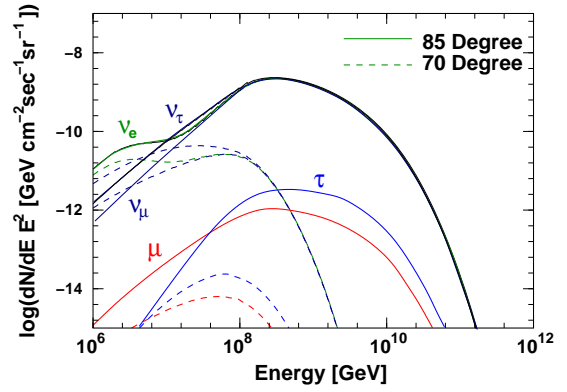


FIG. 3: Fluxes of the EHE particles at the IceCube depth for a scenario of the neutrino production by the GZK mechanism. Two cases in the nadir angle are shown in the figure.

lows larger fluxes which can still be consistent with the EHECR and the EGRET γ -ray observations [24], here we limit the present calculations to the conventional case that the homogeneously distributed astrophysical source are responsible for the observed EHECR flux below 10^{20} eV.

We solve Eqs. 3 and 4 to evaluate the particle fluxes at an underground depth where a kilometer-scale neutrino observatory is expected to be located. The IceCube neutrino telescope is constructed at 1400 m depth below the ice surface and we take this number as a representative depth. It has been found that changing this depth within a factor of two would not affect the overall EHE particle intensity in significant manner and the conclusion remains same. The neutrino oscillation with full mixing is assumed and ν_μ initial flux is identical to that of ν_τ . For the parameters constrained by the SuperK experiment [25], the oscillation probability in the earth in EHE range is negligible, however, and we do not account the oscillation in the present calculation on the propagation.

Fig. 3 shows the fluxes with nadir angle of 85 and 70 degrees, respectively. The initial primary cosmogenic neutrino fluxes are taken from Ref. [21]. Taus notably dominate muons because their heavy mass makes them penetrate the earth and because the decay is less important than interactions for the relevant energy range. The case of nadir angle of 70° exhibits the strong attenuation, however, due to the fact that mean free paths of all the relevant interactions including the weak interactions of neutrinos are by far shorter than the propagation distance. This implies that most of the up-going events in a neutrino observatory are coming from horizontal directions.

ν_τ flux becomes dominating over that of ν_μ in low energy range where the τ decay is significantly more important than interactions. This enhancement is made by $\nu_\tau \rightarrow \tau \rightarrow \nu_\tau$ regeneration process. Note that the small bump of the ν_e spectrum is not the propagation effect but generated primarily by EHECR neutron decay in the space [21, 23].

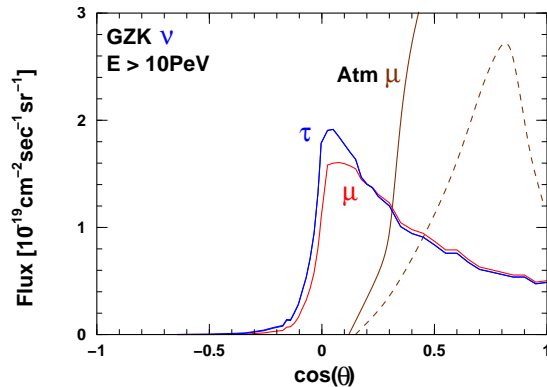


FIG. 4: Dependence of the muon and tau fluxes originated in the cosmogenic neutrinos on the cosine of zenith angle. The integral flux above 10 PeV is plotted in linear scale. The atmospheric muon fluxes are also shown by the solid curve for the conservative estimation with the low energy extrapolation and by the dashed curve for the Corsika-based estimation. The detail of the atmospheric fluxes is discussed in Sec. IV.

The intensity strongly depends on the nadir angle. Fig. 4 shows dependences of the secondary muon and tau fluxes on the zenith angles. Strong attenuation by the earth can be seen but the fluxes are more or less stable in the region of the “downward” events where $\cos \theta \geq 0$. Particles in this range are propagating in ice ($\rho = 0.917 \text{ g/cm}^3$) to enter into the detection volume. We numerically solved the transport equation in the ice medium to derive the downward fluxes. The downward fluxes constitute major fraction of events in an underground neutrino observatory. The detection issues are discussed in Sec. IV.

The energy spectra integrated over zenith angle are shown in Fig. 5. Secondary muons and taus form a potentially detectable bulk with intensity of \sim three order of magnitude lower than the neutrino fluxes. Main energy range is 10 PeV to 10 EeV ($= 10^{10} \text{ GeV}$). Regardless of the neutrino production model, the relative intensity of μ and τ to ν_μ and ν_τ remains approximately unchanged. It should be remarked that intensity of the downward going muons and taus are larger than the upward ones by an order of magnitude. As also seen in Fig. 3, the tau flux dominates over the muons above 10^8 GeV . Enhancement of ν_τ intensity by the regeneration also appears in the upward going trajectories.

The uncertainty in the muon and tau fluxes estimations mainly arises from the fact that we do not know the photonuclear cross sections accurately in EHE range. Fig. 6 shows the comparison of the fluxes with and without photonuclear reactions. Switching off the photonuclear interactions results in a factor of two variance in the intensity.

IV. DETECTION BY A KILOMETER-SCALE NEUTRINO OBSERVATORY

The event rate for a neutrino observatory can be estimated by integrating of the energy spectra shown in Fig. 5 above a threshold energy multiplied by an effective area of the detector which is 1 km^2 in case of the Ice-Cube. The downward events are major contributions and it is necessary to consider the atmospheric muon background, however. The atmospheric muon flux estimation in the relevant energy range is not straightforward because there has been no measurement available and the numerical calculation is also time-consuming as one must fully simulate EHE air shower cascades. Here we use two methods to estimate the flux. One is to extrapolate the calculations in 5 TeV [26] which has been confirmed to be consistent with the measurement. Because the cosmic ray energy spectrum follows $E^{-2.7}$ in TeV region while high energy cosmic ray spectrum above 10 PeV are steeper following E^{-3} , this extrapolation would be overestimating the flux, but it gives the conservative evaluation. Another is to run the Corsika air shower simulation [27] with energy spectrum of the observed E^{-3} and count number of high energy muons reaching to ground. Then we solve the transport equations for the derived muon fluxes at surface. The obtained results of the background intensity in downward events are shown in the right panel of Fig. 5 by two dashed lines. One can see that the muon background spectrum is quite steep. Setting a higher threshold energy, therefore, would be able to eliminate the background contamination. The flux dependence on the zenith angle is shown in Fig. 4 when the threshold energy is 10 PeV. It is clearly seen that the muon background attenuates faster than the neutrino-induced EHE muons and taus, and there is a window where the signals dominate the muon background. Table II summarizes the intensity with threshold energy of 10 PeV for the various EHE neutrino models together with those of the atmospheric muon background.

In fact, what neutrino detectors can measure in direct manner is not energy of muon/tau tracks but energy loss in a detection volume. The relation between energy and energy loss which is described by

$$-\frac{dE}{dX} \simeq \beta E \quad (5)$$

evaluate the energy from the measured energy loss ΔE . Here β is the average inelasticity given by

$$\beta = \int_{y_{\min}}^{y_{\max}} dy' y' \frac{d\sigma}{dy'}. \quad (6)$$

For the e^\pm pair creation of muons in ice, $\beta \simeq 1.3 \times 10^{-6} \text{ cm}^2/\text{g}$. Therefore the average energy loss fraction due to

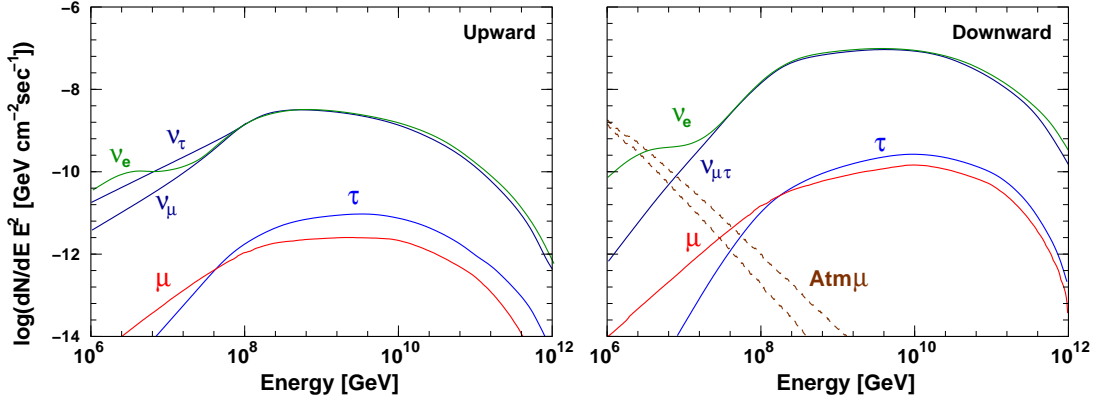


FIG. 5: Energy spectra of $\nu_e, \nu_\mu, \nu_\tau, \mu, \tau$ originated in the cosmogenic neutrinos at the IceCube depth. The intensities are integrated over solid angle and shown for the upward region ($\cos \theta \leq 0$: Left panel) and the downward region ($\cos \theta \geq 0$: Right panel). The two dashed lines represent the atmospheric muon intensities. The upper line shows the conservative estimation based on simple extrapolation from the calculation at 5 TeV while the lower line is derived by the Monte Carlo simulation with the Corsika package.

TABLE II: Integral flux intensities and the event rates for several EHE neutrino models.

	$I_{\nu_{\mu,\tau}}(E \geq 10 \text{ PeV})^a$ [cm ⁻² sec ⁻¹ 2π ⁻¹]	$I_\mu(E \geq 10 \text{ PeV})$ [cm ⁻² sec ⁻¹]	$I_\tau(E \geq 10 \text{ PeV})$ [cm ⁻² sec ⁻¹]	$I_\mu(E_{\text{loss}} \geq 10 \text{ PeV})$ [cm ⁻² sec ⁻¹]	$I_\tau(E_{\text{loss}} \geq 10 \text{ PeV})$ [cm ⁻² sec ⁻¹]
GZK ^b Downward	5.97×10^{-16}	5.90×10^{-19}	5.97×10^{-19}	4.75×10^{-19}	3.28×10^{-19}
GZK Upward	5.97×10^{-16}	3.91×10^{-20}	6.63×10^{-20}	2.57×10^{-20}	2.64×10^{-20}
TD ^c Downward	9.92×10^{-15}	5.48×10^{-18}	5.11×10^{-18}	3.75×10^{-18}	2.94×10^{-18}
Atmospheric μ	-	2.06×10^{-18}	-	1.74×10^{-19}	-
Atmospheric μ^d	-	7.25×10^{-19}	-	5.34×10^{-20}	-

^aIntensity at surface before propagating in the earth.

^bCosmogenic neutrinos with $(m, Z_{\text{max}}) = (4.0, 4.0)$ in Ref. [21].

^cTopological Defects scenario using SUSY-based fragmentation function in Ref. [6]

^dEstimation based on the Corsika simulation

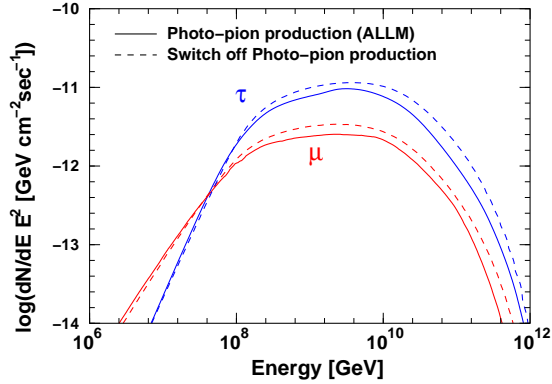


FIG. 6: Dependence of the muon and tau upward fluxes on the photonuclear interactions. The integrated fluxes over nadir angle of 0° to 90° are shown.

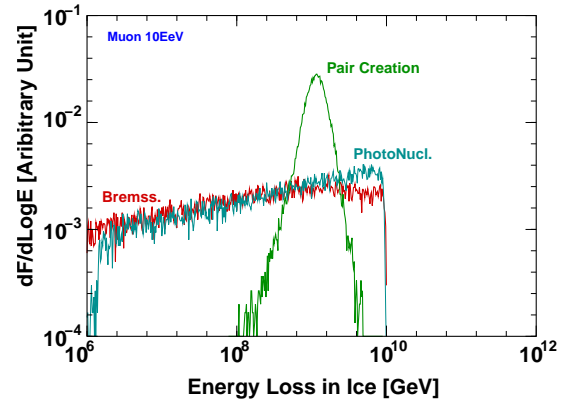


FIG. 7: Distribution of energy-loss in propagation of muons over 1 km in ice. The primary energy of muons is 10^{10} GeV. Contributions from each interaction are shown separately.

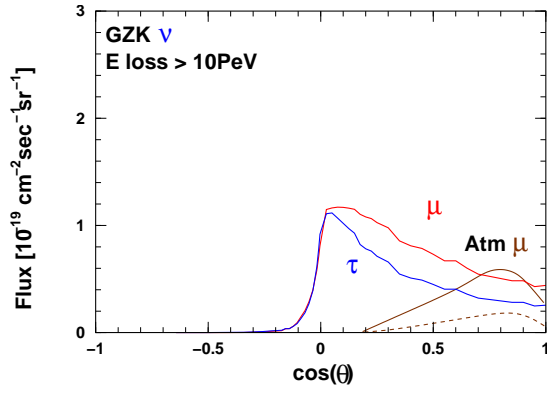


FIG. 8: Dependence of the muon and tau fluxes originated in the cosmogenic neutrinos on the cosine of zenith angle. The integral flux above 10 PeV in the energy loss is plotted in linear scale. The atmospheric muon fluxes are also shown by the solid curve for the conservative estimation with the low energy extrapolation and by the dashed curve for the Corsika-based estimation.

the pair creation is

$$\begin{aligned} \frac{\Delta E}{E} &\simeq \beta^{e^\pm} \Delta X \\ &= 0.12 \left(\frac{\beta^{e^\pm}}{1.3 \times 10^{-6}} \right) \left(\frac{\rho_{ice}}{0.92 \text{ gcm}^{-2}} \right) \left(\frac{\Delta L}{1 \text{ km}} \right) \end{aligned} \quad (7)$$

indicating that 10 % of the muon primary energy is deposited in a detection volume. Because the radiative interactions like Bremsstrahlung have stochastic nature, ΔE is fluctuated significantly in event by event bases, however. We carried out a Monte Carlo simulation to see the fluctuation. The simulation code uses the same cross section and the decay tables but calculates an energy of a particle after an infinitesimal propagation length ΔX with the Monte Carlo method instead of solving the transportation equations. Fig. 7 shows the distribution of the energy loss of muons in running over 1 km in ice. The energy loss distribution due to the pair creation may be narrow enough for the CEL approximation, this is not the case for the distributions due to the other interaction, however. It is not appropriate to approximate the entire distribution by a δ -function, which implies that the energy *loss* rather than the energy would be better to describe the event characteristics.

As more realistic criteria, we introduce the threshold of the energy loss in ice instead of the energy itself. Fig. 8 shows the GZK integral flux dependences on the zenith angle in the case of 10PeV threshold in the energy loss. One can see in comparison to Fig. 4 that the GZK fluxes are larger than or comparable to the muon background intensity in all the zenith directions in this energy-loss-based criteria. It indicates that it is probable that the EHE neutrino search using downward events can be made under almost background-free environment.

It should be noted that the tau flux is lower than the muon flux in this criteria. This is because the heavier

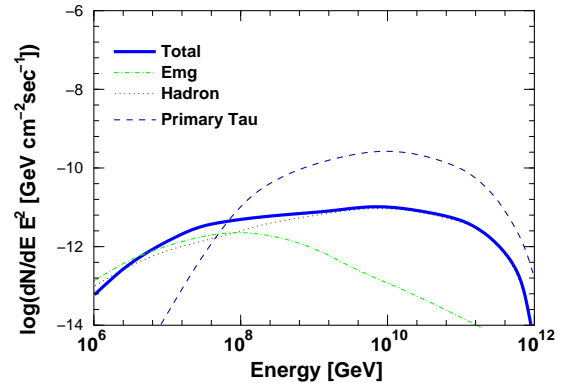


FIG. 9: The tau fluxes at the IceCube depth originated in the cosmogenic neutrinos as a function of energy (the dashed curve), total energy loss in ice (the solid curve), energy loss in form of electromagnetic cascades (the dash-dot curve), and that in form of hadronic cascades (the dotted curve).

mass of tau suppresses the energy loss compared to that of muons with same energy. This situation is illustrated in Fig. 9 where the tau fluxes are plotted as functions of energy and energy loss in ice during 1km propagation. The intensity above 10^7 GeV is reduced because of the energy loss suppression. The higher energy loss takes place in form of the hadronic cascades initiated by the photonuclear interaction. Table II lists the intensity of muon and tau above 10 PeV of energy loss for the fluxes of the cosmogenic [21] and top-down model [6]. The event rate under this criteria is found to be $0.27 (\mu + \tau)/\text{km}^2$ year for the cosmogenic neutrino fluxes with the moderate source evolution. Note that the downward event rate is $0.25 / \text{km}^2$ year and dominates in the overall rate.

The IceCube sensitivity on EHE neutrinos can be evaluated by the event rate per energy decade $dN/d\text{Log}E$. For a given energy of primary neutrinos, the secondary muon and tau fluxes are calculated by the transport equations Eqs. 3 and 4 as a function of zenith angles. The probability that energy loss with the threshold value or greater occurs are estimated by the Monte Carlo simulation and convoluted with the flux integration over energy and zenith angle to give the rate. Fig. 10 shows the resultant sensitivity by the IceCube detector with 1 km^2 detection area. The various model predictions are also shown for comparison. The 90 % C.L. upper limit *i.e.*, 2.3 event/energy decade/10 year is plotted for different threshold of the energy loss. The ν_μ sensitivity is better below 10^8 GeV region because their energy loss is larger than that of taus with same energy, but the tau decay which results in large energy deposit in a detection volume make dominant contributions in the ν_τ sensitivity in this relatively low energy range forming a slight bump structure in the sensitivity curve. The 90 % C.L. upperlimit of EHE neutrino fluxes by a km^2 detection area would be placed at $E^2 dF/dE \simeq 3.7 \times 10^{-8} \text{ GeV/cm}^2 \text{ sec sr}$ for ν_μ and 4.6×10^{-8} for ν_τ with energies of 10^9 GeV in absence of signals with energy-loss in a detection volume

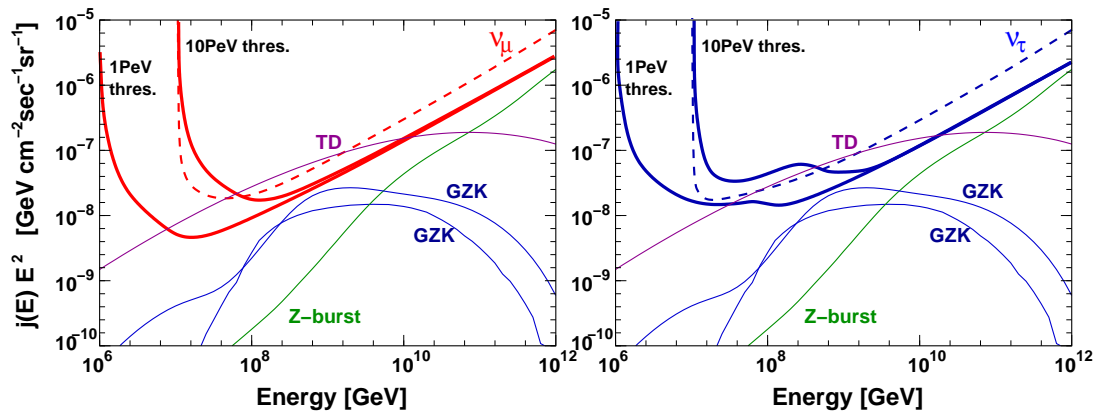


FIG. 10: The IceCube sensitivities on the EHE neutrino fluxes. 90 % C.L. limits by a 1km^2 detection area with 10 years observation are drawn. The left panel shows the case of ν_μ and the right panel shows the ν_τ case. Labels refer to GZK ([21] for the lower curve, [24] for the upper curve), TD [6], and Z-burst [30]. The dashed curves show the sensitivities by events of neutrinos interacting inside the detector volume.

of 10PeV or greater.

This bound would not exclude the cosmogenic neutrino production model but strongly constrain the cosmic ray injection spectrum in the model. Cosmic ray nucleon injection spectra harder than $E^{-1.5}$ would violate the bound [24]. On the other hand, as long as the injection spectra is softer than E^{-2} , which is very likely in case of the astrophysical cosmic ray sources, the IceCube bound would less constrain the source evolution as seen in Fig. 10 where we plotted an extreme scenario of the cosmological evolution $(1+z)^5$ where z is the redshift [24]. Stronger evolution possibilities than this case are inconsistent with the diffuse background γ -ray observation by EGRET [28] since the GZK mechanism also initiated the electromagnetic cascades [21, 22, 24] via photoproduced π^0 decay and e^\pm pair creation by EHECRs collisions with the CMB photons, forming the photon flux below 100 GeV which is constrained by the observation.

The topological defects scenario, on the other hand, would be severely constrained by absence of EHE event detection by the IceCube. The expected event rate is ~ 2 events/year km^2 as one can calculate from Table II. The expected EHE neutrino flux in the Z-burst model [29], the scenario that the collisions of EHE neutrinos with the cosmological background neutrinos to explain the EHECR fluxes without the GZK cutoff, is well below the IceCube bound if the injection neutrino spectrum is E^{-1} as described in Ref. [30].

Although less significant, there are μ and τ events produced by neutrinos *inside* the detector instrumented volume. In this case the produced charged leptons propagate only a part of the observation volume. We carried out the same Monte Carlo simulation deriving the results of Fig. 7 but in which ν_μ and ν_τ were initially entering into the ice volume. The probability that neutrinos interact inside the 1 km^3 volume and that the produced muon or tau losses its energy greater than 10 PeV were estimated and convoluted with the neutrino intensity at

the IceCube depth. The detection sensitivities by this channel are shown in thick dashed curves in Fig. 10. In the EHE regime above $\sim 10^8$ GeV, the intensity of internally produced muon and tau events is too small to contribute the overall sensitivity because the neutrino target volume is limited by the size of the detector *i.e.* 1 km^3 . Below 10^8 GeV, on the other hand, including this channel improves the sensitivity in sizable manner because the energy losses of muons and taus during their propagation over long distances are more likely to transfer them out of the energy range above the 10 PeV threshold, which leads to reduction of the effective neutrino target volume for producing EHE muons and taus outside the detector volume. There is little gain in EHE neutrino searches, however, because the proposed EHE neutrino models have its main energy range above 10^8 GeV.

V. SUMMARY AND OUTLOOK

We calculated propagation of the EHE neutrinos and charged leptons in the earth to derive their intensities and their dependence on nadir angles. The secondary produced muons and taus form detectable fluxes at the IceCube depth, with intensity of three order of magnitude lower than the neutrino fluxes. The realistic criteria, requiring energy deposit greater than 10 PeV in 1 km^3 volume of ice, leads to ~ 0.27 events/year for the cosmogenic neutrinos in case of the moderate source evolutions. The topological defects scenario would be severely constrained.

The atmospheric muon background are likely to be negligible even for downgoing events. The background rate is ~ 0.05 event/ km^2 year. It should be noted that we ignored the possible contributions of prompt muons from the charm decay in EHE cosmic ray air showers [31], however. The atmospheric muon intensity can be increased

by an order of magnitude but a large uncertainty remains due to highly uncertain cross sections in the charm production. The energy spectrum of the prompt muons would still be much steeper than the expected spectrum in the proposed EHE cosmic neutrino models, however, and even if the charm production are significant in EHE range, one can easily distinguish the signal detections from the prompt muon background events if the neutrino observatory has reasonable resolution for the energy loss of muons and taus tracks. The detector resolution issues require the detailed detector Monte Carlo simulations for further investigations. The AMANDA experience in relatively low energy muon reconstruction would lead to energy resolution of $\Delta \text{Log } E \simeq 0.3$ [32]. The development of the detector Monte Carlo simulation is under progress and its application to the present results will be important future work toward the search for EHE neutrinos by

the IceCube observatory.

Acknowledgments

We wish to acknowledge the IceCube collaboration for useful discussions and suggestions. We thank Dmitry Chirkin and Thomas Gaisser for helpful discussions on the atmospheric muon issues. Special thanks go to Mary Hall Reno for providing the cross section table evaluated by the CTEQ version 5 parton distribution. This work was supported in part by the Grants-in-Aid (Grant # 15403004 and 15740135) in Scientific Research from the MEXT (Ministry of Education, Culture, Sports, Science, and Technology) in Japan.

-
- [1] for a review see, e.g., M. Nagano and A. A. Watson, Rev. Mod. Phys. **72**, 689 (2000); J. W. Cronin, Rev. Mod. Phys. **71**, S165 (1999); S. Yoshida and H. Dai, J. Phys. G: Nucl. Part. Phys. **24**, 905 (1998).
 - [2] V. S. Beresinsky and G. T. Zatsepin, Phys. Lett. **28B**, 423 (1969).
 - [3] K. Greisen, Phys. Rev. Lett. **16**, 748 (1966); G. T. Zatsepin and V. A. Kuzmin, Pisma Zh. Eksp. Teor. Fiz. **4**, 114 (1966) [JETP. Lett. **4**, 78 (1966)].
 - [4] P. Bhattacharjee, C. T. Hill, and D. N. Schramm, Phys. Rev. Lett. **69**, 567 (1992).
 - [5] G. Sigl, S. Lee, D. N. Schramm, and P. S. Coppi, Phys. Lett. B **392**, 129 (1997).
 - [6] G. Sigl, S. Lee, P. Bhattacharjee, and S. Yoshida, Phys. Rev. D **59**, 043504 (1999).
 - [7] J. Alvarez-Muñiz and F. Halzen, Phys. Rev. D **63**, 037302 (2001).
 - [8] J. Jones, I. Mocioiu, M. H. Reno, and I. Sarcevic, hep-ph/0308042.
 - [9] J. L. Feng, P. Fisher, F. Wilczek, and T. M. Yu, Phys. Rev. Lett. **88**, 161102 (2003); K. Giesel, J. -H. Ju-reit and E. Reya, Astropart. Phys. **20**, 335 (2003).
 - [10] S. Yoshida, Proc. of the 28th ICRC, H.E.2.3, 1369 (2003); <http://icecube.wisc.edu/>.
 - [11] S. Kelner, R. P. Kokoulin, A. A. Petrukhin, Phys. At. Nucl. **63**, 1603 (2000).
 - [12] R. P. Kokoulin and A. A. Petrukhin, Proc. of the 12th ICRC (Hobart) Vol.6 p.A2436 (1971); S. R. Kelner, R. P. Kokoulin, and A. A. Petrukhin, Phys. At. Nucl. **62**, 1894 (1999).
 - [13] Yu. M. Andreev, L. B. Bezrukov, and E. V. Bugaev, Phys. At. Nucl. **57**, 2066 (1994); S. R. Kelner, R. P. Kokoulin, and A. A. Petrukhin, Phys. At. Nucl. **60**, 576 (1997); I. A. Sokalski, E. V. Bugaev, and S. I. Klimushin, Phys. Rev. D **64**, 074015 (2001).
 - [14] S. Iyer Dutta, M. H. Reno, I. Sarcevic, and D. Seckel, Phys. Rev. D **63**, 094020 (2001).
 - [15] H. Abramowicz and A. Levy, hep-ph/9712415.
 - [16] R. Gandhi, C. Quigg, M. H. Reno, and I. Sarcevic, Astropart. Phys. **5**, 81 (1996); Phys. Rev. D **58** 093009 (1998).
 - [17] CTEQ Collaboration, H. Lai *et al.*, Phys. Rev. D **55**, 1280 (1997).
 - [18] T. K. Gaisser, *Cosmic Rays and Particle Physics*, (Cambridge University Press, Cambridge, England, 1990).
 - [19] S. Iyer Dutta, M. H. Reno, I. Sarcevic, Phys. Rev. D **62**, 123001 (2000).
 - [20] A. M. Dziewonsky and D. L. Anderson, Phys. Earth. Planet. Inter **25**, 297 (1981); S. V. Panasyuk, <http://cfauvcs5.harvard.edu/lana/rem/index.html>.
 - [21] S. Yoshida and M. Teshima, Prog. Theor. Phys. **89**, 833 (1993).
 - [22] R. J. Protheroe and P. A. Johnson, Astropart. Phys. **4**, 253 (1996).
 - [23] R. Engel, D. Seckel, T. Stanev, Phys. Rev. D **64**, 093010 (2001).
 - [24] O. E. Kalashev, V. A. Kuzimin, D. V. Semikoz, and G. Sigl, Phys. Rev. D **66**, 063004 (2002).
 - [25] SuperKamiokande Collaboration, Y. Fukuda *et al.*, Phys. Rev. Lett. **85**, 3999 (2000).
 - [26] V. Agrawal, T. K. Gaisser, P. Lipari, and T. Stanev, Phys. Rev. D **53**, 1314 (1996).
 - [27] D. Heck *et al.*, Report FZKA **6019**, (Forschungszentrum Karlsruhe 1998).
 - [28] P. Sreekumar *et al.*, Astrophys. J. **494**, 523 (1998).
 - [29] D. Fargion, B. Mele, and A. Salis, Astrophys. J. **517**, 725 (1999); T. J. Weiler, Astropart. Phys. **11**, 303 (1999).
 - [30] S. Yoshida, G. Sigl, and S. Lee, Phys. Rev. Lett. **81**, 5505 (1998).
 - [31] See e.g., T. S. Sinogovskaya and S. I. Sinogovskiy, Phys. Rev. D **63**, 096004 (2001), and references therein.
 - [32] IceCube Collaboration, J. Ahrens *et al.*, astro-ph/0305196, Accepted for publication in Astropart. Phys.